Carbon Letters
https://doi.org/10.1007/s42823-024-00759-5

Online ISSN 2233-4998
Print ISSN 1976-4251

ORIGINAL ARTICLE

Simultaneous electrochemical detection of ascorbic acid, dopamine and uric acid using Au decorated carbon nanofibers modified screen printed electrode

P. Sakthivel[1] · K. Ramachandran[1] · K. Maheshvaran[2] · T. S. Senthil[3] · P. Manivel[3]

Received: 27 March 2024 / Revised: 25 May 2024 / Accepted: 31 May 2024

Abstract

Gold nanoparticles (Au NPs) decorated carbon nanofibers (CNFs) have been prepared by an electrospinning approach and then carbonized. The prepared Au-CNFs were employed to modifying a screen printed electrode (SPE) for simultaneous determination of ascorbic acid (AA), dopamine (DA) and uric acid (UA). Au NPs are uniformly dispersed on carbon nanofibers were confirmed by the structure and morphological studies. The modified electrodes were tested in cyclic voltammetry (CV), differential pulse voltammetry (DPV) and chronoamperometry (CA) to characterize their electrochemical responses. Compared to bare SPE, the Au-CNFs/SPE had a better sensing response to AA, DA, and UA. The electrochemical oxidation signal of AA, DA and UA are well separated into three distinct peaks with peak potential separation of 280 mV, 159 mV and 439 mV between AA-DA, DA-UA and AA-UA respectively in CV studies and the corresponding peak potential separation in DPV studies are 290 mV, 166 mV and 456 mV. The Au-CNFs/SPE has a wide linear response of AA, DA and UA in DPV analysis over the range of 5–40 μM ($R^2 = 0.9984$), 2–16 μM ($R^2 = 0.9962$) and 2–16 μM ($R^2 = 0.9983$) with corresponding detection limits of 0.9 μM, 0.4 μM and 0.3 μM at S/N = 3, respectively. The developed modified SPE based sensor exhibits excellent reproducibility, stability, and repeatability. The excellent sensing response of Au-CNFs could reveal to a promising approach in electrochemical sensor.

✉ P. Manivel
maninano@gmail.com

[1] Department of Chemistry, Builders Engineering College, Tiruppur 638 108, Tamil Nadu, India

[2] Department of Physics, Kongu Engineering College, Erode 638 060, Tamil Nadu, India

[3] Centre for Nanotechnology, Erode Sengunthar Engineering College, Erode 638 057, Tamil Nadu, India

Published online: 11 June 2024

Graphical abstract

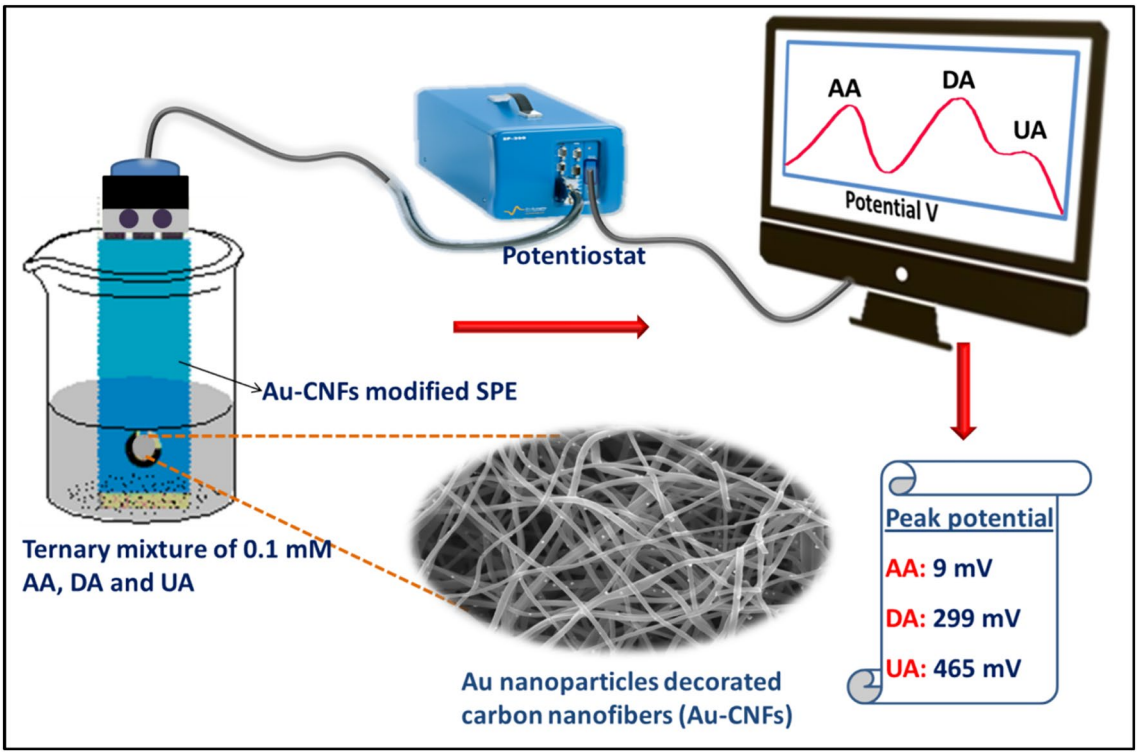

Keywords Gold nanoparticles · Carbon nanofibers · Screen printed electrode · Ascorbic acid · Dopamine · Uric acid

1 Introduction

The current needs on healthcare necessitate rapid and precise biochemical substance screening or detection in order to manage long-lasting illnesses. The human body contains several biochemical compounds, it is essential to detect or analyse these molecules simultaneously in order to screen for diseases [1]. Ascorbic acid (AA), dopamine (DA) and uric acid (UA) were the three primary macromolecules of humans that are directly associated with the biological activity of organisms [2, 3]. AA is commonly used in large scale as an antioxidant in food, animal feed, pharmaceutical formulation and cosmetic applications [4]. DA is a neurotransmitter and plays a very important role in the function of central nervous, renal, hormonal and cardiovascular systems [5]. UA is the major final product of urine catabolism in human body. In a healthy human, the normal level of UA in urine is in milli molar range, whereas in serum, it is in micro-molar range [6]. Unexpected variations of AA, DA, and UA could bring substantial risks in human, like such as cancer, diabetes mellitus, hepatic disorders, Parkinson disease, hyperuricaemia, pneumonia and kidney stones [7–9]. Consequently, it is necessary for designing a quick and efficient sensing system that can simultaneous detect these three compounds with great sensitivity as well as high selectivity.

Over the last several years, various approaches were established for the examination of chemical and biological substances [10–14]. The electrochemical analysis is the most frequently employed to directly detect DA, AA, and UA due to their assistances of quick response, inexpensive, simple setup, and a broad spectrum of application [15]. But the similarity of DA, AA, and UA oxidation signal potentials makes it impossible to determine three substances simultaneous on bare electrodes [16]. To address this limitation, significant attempts have been undertaken to create modified electrodes containing a type of metal nanoparticle. The several precious metallic nanoparticles, like platinum (Pt) silver (Ag) and gold (Au) are frequently employed as enhancing the electrochemical response of sensors because of their durability, electron transport and biocompatibility [17–19]. Au nanoparticles, a developing precious metal nanoparticle, have gained popularity among researchers in recent times due to their greater quantity and resistance to hazardous intermediary substances [20–22]. However, the agglomeration of Au nanoparticles (Au NPs) must be fully controlled before large use in electrode construction. Plenty of focus

has been associated for the dispersion of nanoparticles to prevent agglomeration utilizing low-dimensional carbon materials, like reduced graphene oxide, carbon nanotubes and carbon nanofibers, because of their significant physical and chemical properties [23–25]. The CNFs possesses super high surface area, increased specific strength and structural adaptability, which could serve as perfect substrate or carrier for dispersing Au nanoparticles [26–28]. Because of their high mechanical strength, electrical conductivity, and chemical stability, carbon nanofibers (CNFs) have always been used as electrodes in supercapacitors, secondary batteries, hydrogen evolution, and sensors [29, 30]. Also, the CNFs are able to promote the kinetics of electron transfer reaction, minimize electrode surface fouling and enhance electrocatalytic activity [31].

To integrate sensing tools into the electrochemical point-of-care system, some criteria must be fulfilled, such as electrochemical cell integration and scaling down, minimum sample usage, and reusable operation [32]. Screen printed carbon electrode (SPE) provide significant advantages in terms of flexibility, surface area, durability and volume of electrolyte during the process. Furthermore, compared to three separate electrodes, they provide a favourable approach for easily operations of electrochemical analysis with comprise of a working, counter, and reference electrode coated using screen printing methodology [33, 34]. The potential window, low background current and simplicity of this surface modification electrode system makes it a perfect sensor for the electrochemical investigation of many substances [35]. Biosensors, such as those for glucose, uric acid, and dopamine have been designed for clinical biomarker detection using SPE which acting as base transducers in the sensing process [36–39]. The combination of Au NPs and CNFs not only overcomes the aggregation of Au NPs, but also improves electrocatalytic activity of SPE modified with Au-CNFs complex. However, the electrocatalytic activities of Au NPs with carbon nanomaterials have been rarely studied. Recently, Cheng et al. prepared a novel electrochemical sensing platform for detection of dopamine based on gold nanobipyramid/multi-walled carbon nanotube hybrids [21]. Kavya et al. developed a voltammetric sensor for determination of acetaminophen using glassy carbon electrode modified by gold nanofibers decorated iron metal–organic framework nanocomposite [40]. However, as far as we know, there are no reports on highly selective, sensitive and simultaneous detection of AA, DA and UA in their ternary mixture by Au-CNFs/SPE.

In this work, Au NPs decorated CNFs (Au-CNFs) were prepared using an electrospinning approach and then carbonized. The high sensitivity and selectivity were achieved in simultaneous detection of AA, DA, and UA using the Au-CNFs modified SPE. The electrochemical activity of Au-CNFs/SPE was examined by using CV, DPV and CA technique. The constructed simple and adaptable sensor offers a promising solution for simultaneous detection of biomolecules in the human body.

2 Experimental section

2.1 Materials

Polyacrylonitrile (PAN, Mw = 150 000 g mol^{-1}), N,N-dimethylformamide (DMF 99%), Gold (III) chloride trihydrate ($HAuCl_4 \cdot 3H_2O$ 99%), AA 99%, DA 98% and UA 99% were purchased from Sigma-Aldrich. The commercial zensor screen printed electrode was purchased from CH Instruments (ALS electrode accessories). Sodium dihydrogen phosphate (NaH_2PO_4, 99.0%), and disodium hydrogen phosphate (Na_2HPO_4, 99.0%) were obtained from Himedia Laboratory. All the analytical-reagent grade chemicals were used without further purification. Phosphate buffer solution (PBS 0.1 M) with pH value 7.2 was prepared with the mixed solution of NaH_2PO_4 and Na_2HPO_4. The de-ionized water was utilized to make aqueous medium for entire experiments.

2.2 Preparation of Au NPs decorated CNFs

The uniform and bead-free electrospun Au NPs adorned CNFs were made using a conventional method, which were then carbonized [41]. The PAN (13 wt%) was dissolved in DMF and stirring at room temperature until it formed a clear solution. Then, 0.130 g $HAuCl_4 \cdot 3H_2O$ was put into the above solution and agitated for 12 h. The obtained to a homogeneous solution was then filled in dispenser and connected to a dispenser pumping machine (KDS 101). The metal ion solution flows was adjusted to 0.5 mL/hour using a dispenser system. The conductive metal collector have been placed 15 cm from the dispenser needle tip and covered with aluminum foil. A high-voltage power source was used to apply an electric field of 10 kV. The entire electrospinning procedure was done at room temperature with in a polycarbonate chamber. The prepared Au^{3+} ions loaded PAN nanofibers was collected and placed in a fume hood for 12 h to remove any residual solvent. Subsequently, the above nanofiber mat has been pre-treated in the tubular furnace for 2 h at 250 °C with heating flow rate of 2 °C min^{-1} under environment condition. Afterwards, the pre-treated nanofibrous mat was carbonized in N_2 atmosphere for 3 h at 900 °C with a heating flow rate of 5 °C min^{-1}. PAN nanofibers were converted to CNFs through the carbonizing process. Concurrently, Au^{2+} ions turned into Au NPs, which were subsequently mostly inserted into the CNFs. The resulting nanofiber mats were called CNFs and Au-CNFs. Scheme 1 depicts the complete preparation procedure for Au NPs decorated CNFs.

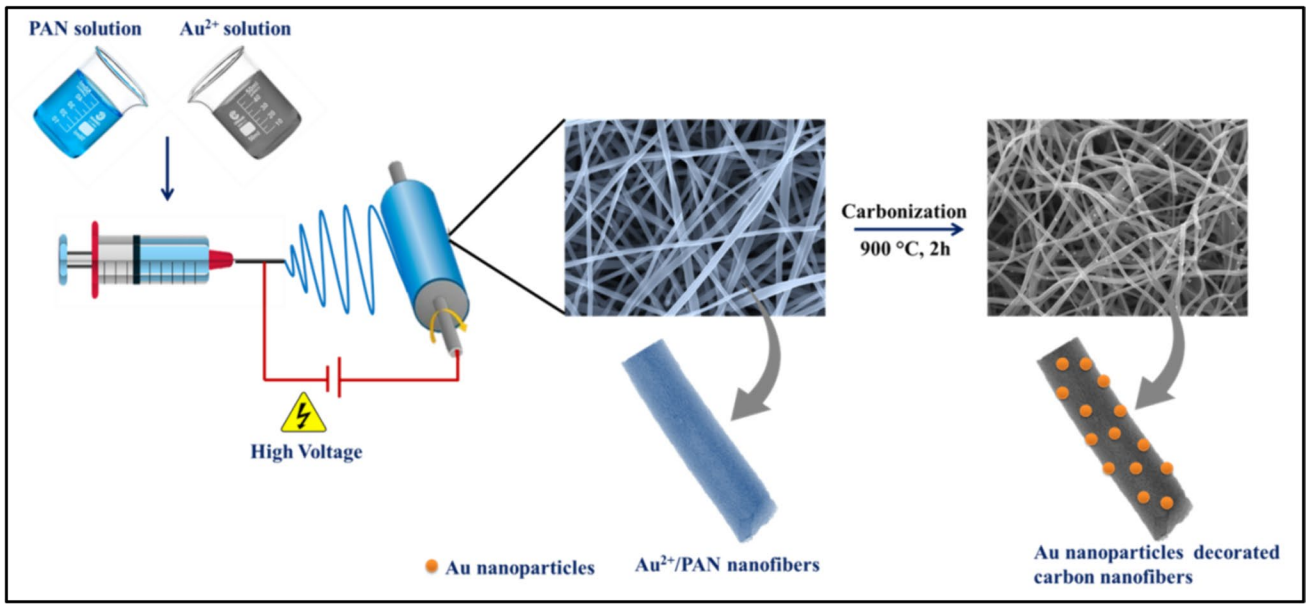

Scheme 1 A schematic illustration for the preparation of Au NPs decorated CNFs by electrospinning technique

2.3 Characterizations of Au NPs decorated CNFs

The morphological features of the Au-CNFs have been investigated using Carl Zeiss FE-SEM in conjunction with Energy Dispersive X-ray spectroscopy (XPS, Thermo Scientific, ESCALAB 250). The dimensions and diameters of the Au NPs on CNFs were explored by Transmission Electron Microscopy (TEM-JEOL, JEM 2010). Further, the formations along with characteristic binding energy of Au-CNFs were examined through X-ray photoelectron spectroscopy (XPS) techniques. The CV experiments and EIS were performed using a three-electrode setup BioLogic (SP-300) electrostatic system. The electrochemical behaviour of Au-CNFs/SPE studied using CV at a scan rate of 20 mV s^{-1} within the potential range from − 0.2 to + 0.8 V vs. Ag/AgCl in the aqueous solution of 0.5 M H_2SO_4 electrolyte.

2.4 Preparation of Au-CNFs modified SPE electrode

The precise amount of Au-CNFs has been suspended in ethanol to produce modifier slurry of 1 mg/ml. The prepared slurry solution was subjected to ultra-sonicated for 15 min at room temperature. Au-CNFs/SPE was constructed by drop casting 5 µL of dispersed Au-CNFs solution on the working area of SPE along with Nafion solution and dried at ambient temperature as shown in Scheme 2. Also, the CNFs/SPE was prepared for comparison using a similar process. The 0.1 M PBS (pH 7.2) was used to perform all electrochemical measurements. The parameters of CV and DPV experiment were set as following for detection of AA, DA and UA. CV settings: potential range: − 0.2 to + 0.8 V; scan rate: 50 mV s^{-1} and DPV settings: step potential: 5 mV; amplitude: 60 mV; pulse width: 0.05 s; sample width: 0.01 s and pulse period: 0.2 s.

3 Results and discussion

X-ray photoelectron spectroscopy (XPS) measurement is performed to investigate the chemical composition and surface atomic states of the as-prepared CNF and Au-CNFs. Generally, the XPS spectra further analysed the presence of Au element in the sample. Figure 1a displays the survey spectrum of CNFs and Au-CNFs from 0 to 1000 eV together with the four unique peaks of Au, C, N, and O elements of the prepared sample. As seen in Fig. 1b, the C 1 s peaks of Au-CNFs were de-convoluted into four distinct peaks, including the prominent peak found at 284.7 eV, suggesting that the primary sp^2 carbon bonds of CNFs [42]. Also found were the following: sp^3 carbon bonds (C–H) at 285.5 eV, C–O bonds at 286.3 eV, and C = O bonds at 287.7 eV [43, 44]. The de-convoluted N 1 s spectra reveals three distinct peaks at 398.1 (pyridinic N), 400.9 (pyrrolic N), and 402.5 eV (graphitic N) as demonstrated in Fig. 1c [45]. As seen in Fig. 1d, the Au 4f signal of Au-CNFs shows two significant signals at 84.0 and 87.7 eV, resultant to the spin–orbit splitting doublets Au $4f_{7/2}$ and Au $4f_{5/2}$, respectively. Moreover, the de-convoluted spectra revealed the presence of two chemically distinct Au elements with metallic Au^0 (84.1 and 87.2 eV) and Au^+ oxide (84.9 and 88.6 eV) [46]. No obvious separate satellite peaks were observed in

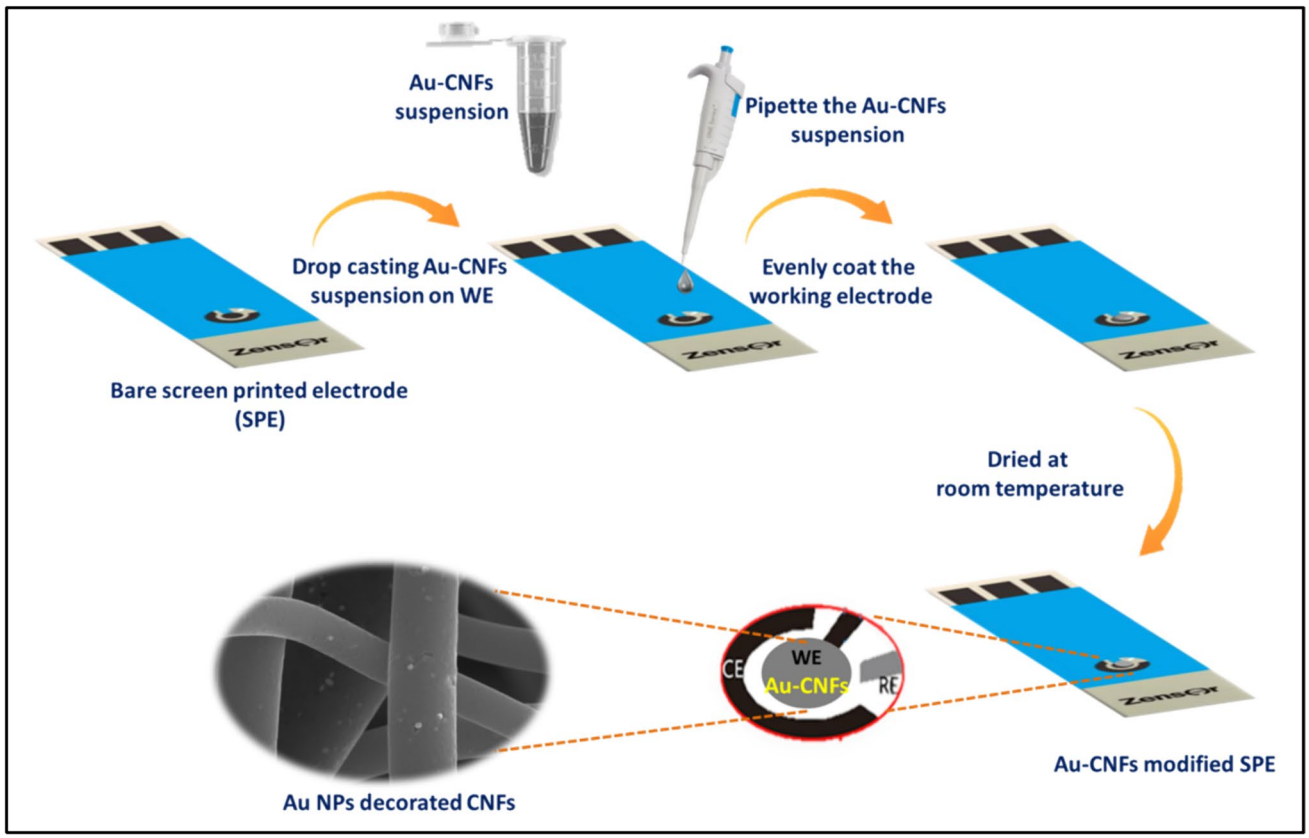

Scheme 2 Schematic illustration for the construction of Au-CNFs modified SPE by direct drop casting method

all of the XPS spectra, demonstrating that several carbon layers on the surface of the Au NPs are effective in protecting the Au from electro-oxidation. Based on the XPS results, we concluded that the Au NP-decorated CNFs were predominantly metallic.

FE-SEM was used to examine the morphologies of electrospun bare CNFs and Au NPs decorated CNFs. Figure 2 shows the FE-SEM images of CNFs, and Au-CNFs. It clearly shows that the smooth surface nanofibers were observed without beads and damages, demonstrating the very good spinning conditions of the precursor mixture. The average diameter of bare and as-prepared Au-CNFs is around 100–200 nm. In general, the diameter of nanofibers is directly related to the surface tension of electrospinning precursor. In this case, a higher voltage is needed to balance or control the surface tension due to the presence of metal chloride in the electrospinning solution [47]. However, the higher voltage could result in a smaller diameter during the electrospinning process. For that reason, the suitable solid weight of Au^{3+} salt in our work has been adjusted to 1% Au for PAN weight. Typically, PAN nanofibers were transformed into carbon nanofibers under the condition of N_2 atmosphere, and Au^{3+} ions were reduced simultaneously and formed into Au NPs. The Au NPs were directly produced and densely grown on the whole surface of CNFs without aggregation, as seen in Fig. 2c and d. The size of the Au NPs ranges from 10 to 20 nm. Further, the Au-CNFs exhibit distinct nanofiber morphology and integrated networks, forming the 3D architectures. The close proximity promotes effective electron transfer between nanoparticles and CNFs, which is crucial to the higher electrocatalytic performance of Au-CNFs. Moreover, the existence elements of C, O, and Au were confirmed by the energy dispersive X-ray spectrum (EDX) analysis as shown in Fig. 2e. The specific peaks of Au element also show the presence of Au NPs on the surface CNFs. The Au-CNFs exhibited more surface roughness than bare CNFs due to the direct formation of Au NPs on CNFs. It could increase the surface area and active sites of Au-CNFs, which would enhance their electrochemical activity for analyte oxidation [48].

To further investigate the size and shapes of Au NP decorated CNFs using TEM analysis. Figure 3a and b shows TEM images of bare CNFs following the carbonization procedure. The bare CNFs exhibited a smooth, transparent surface and a diameter around 200 nm. Further, Fig. 3c and d illustrates the Au NPs decorated CNFs and it is clearly observed that similar size (~ 10 nm) of sphere Au NPs are evenly distributed on the CNFs. In addition, HR-TEM

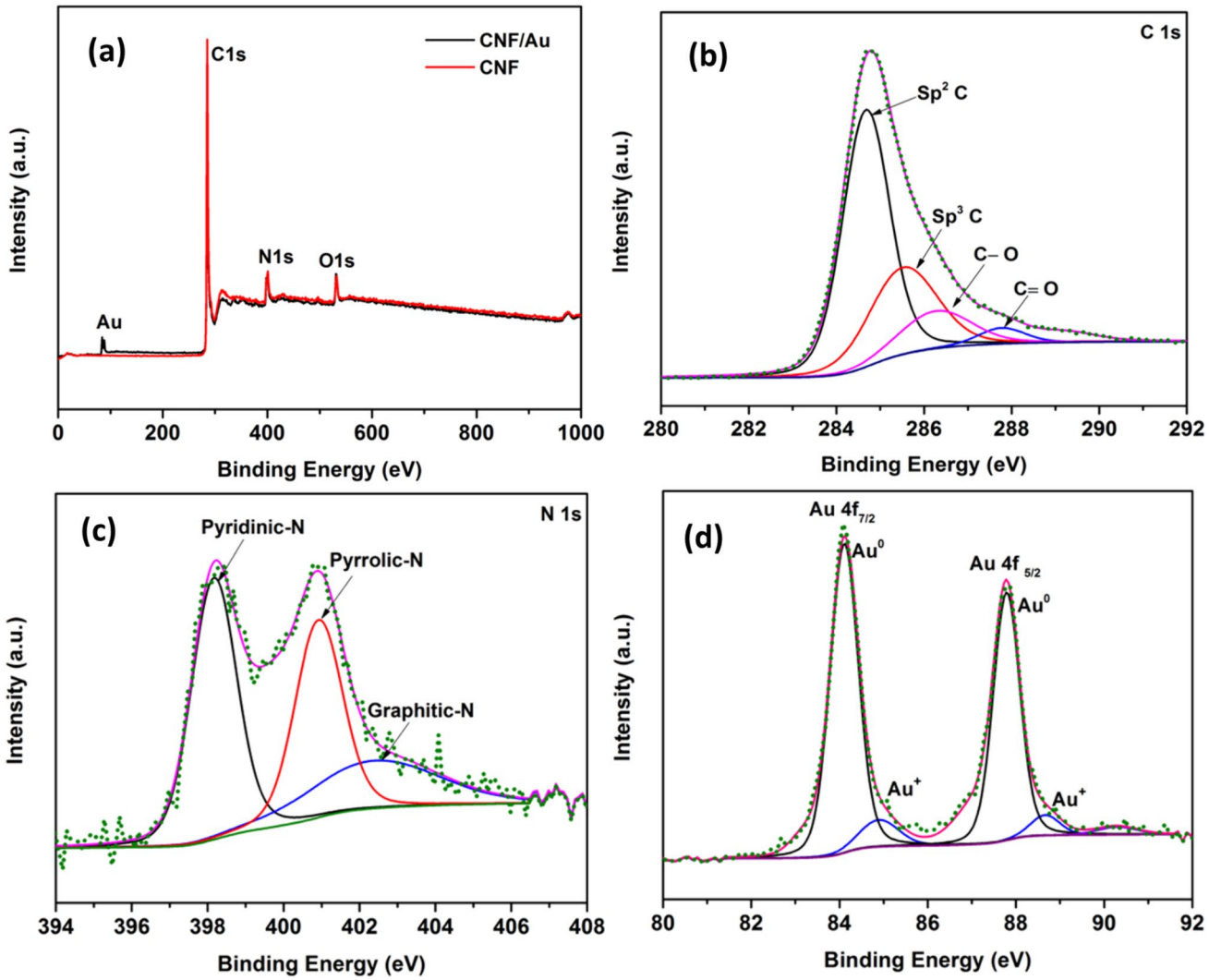

Fig. 1 XPS spectra of prepared Au-CNFs for **a** survey spectrum, **b** C 1s, **c** O 1s and **d** Au 4f

images were further analysed to confirm the crystallinity of Au NPs on the CNFs surface. Inset Fig. 3d shows clear lattice fringes indicating the high crystallinity of Au NPs. The measured d space value for 0.22 nm matches with the 111 planer in the FCC structure of Au [49]. Similarly, Au NPs have been distributed on the CNFs and are hard to remove from the CNFs, indicating that materials sustainability. Also, the carbon shell layer can protect the Au NPs from the oxidation and corrosion during the electrochemical process. The enhanced interaction between Au NPs and CNFs allows electron transfer and enhance the electrochemical activity. All these characterization results demonstrate the expected Au-CNFs are prepared successfully.

3.1 Electrochemical behaviour of Au-CNFs/SPE

The electron transfer kinetics and electrocatalytic activity of Au-CNFs/SPE was examined using CV in 0.5 M H_2SO_4 medium. The mass of the CNFs and Au-CNFs are kept constant on each modified SPE. As illustrated in Fig. 4a, the redox peaks were significantly enhanced at the Au-CNFs/SPE as compared with those of CNFs/SPE and bare SPE. This could be ascribed to the significant properties with accelerating electron transfer of the Au-CNFs, which leads to improved electrochemical performance. Furthermore, it is obvious that Au-CNFs modified SPE exhibited the strong oxidation peak at 350 mV and peak current (5.42 mA) as compared to bare SPE. The minimum potential value and higher peak current response of Au-CNFs/SPE revealed that the Au-CNFs performed efficiently for electron transfer. Moreover, the increased electrochemical properties of Au

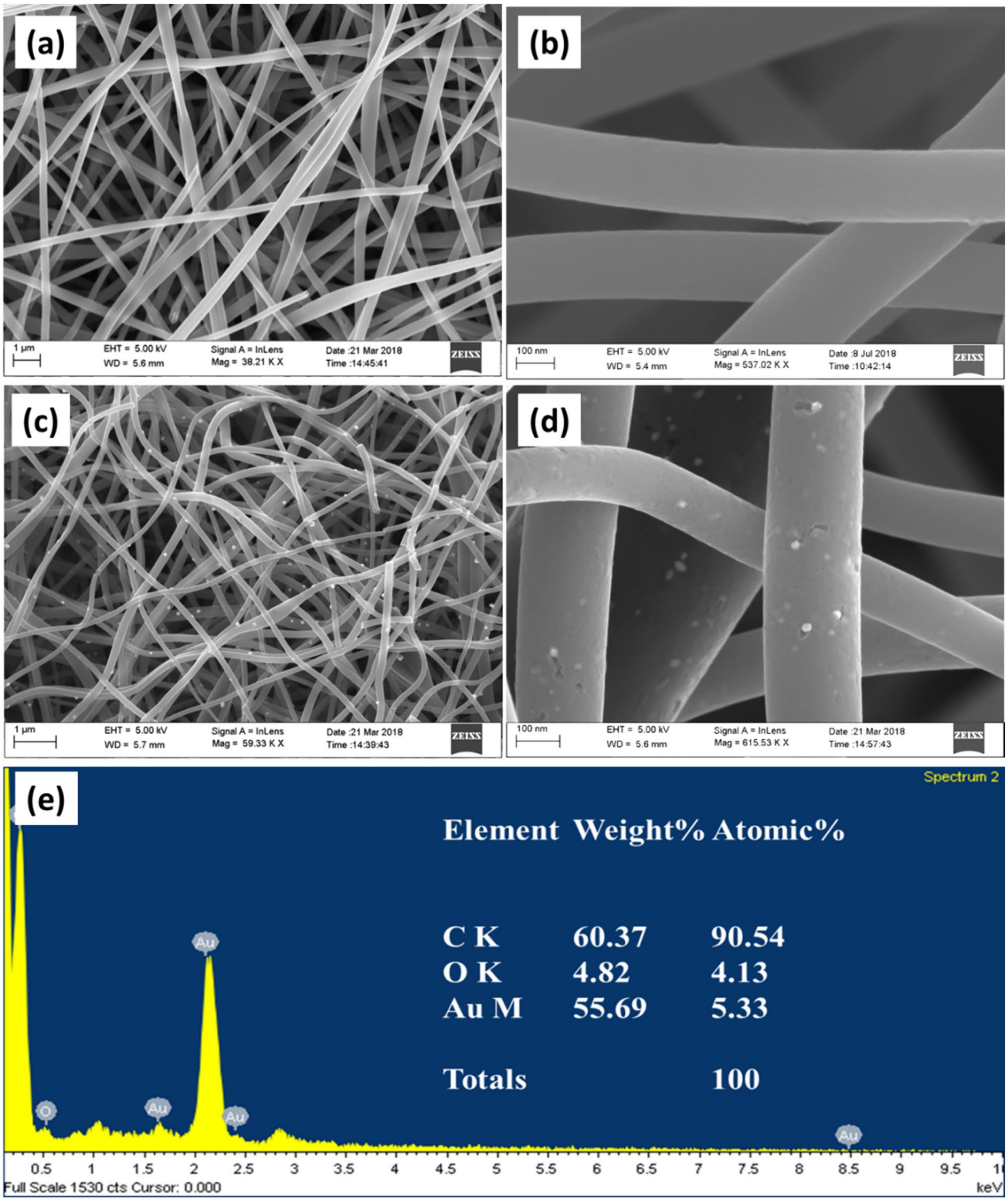

Fig. 2 FE-SEM images of **a** & **b** CNFs, **c** & **d** Au-CNFs and **e** EDS spectra of Au-CNFs

NPs decorated CNFs were enhanced the significant electrochemical performance of the modified electrode [22]. Further, Fig. 4b shows the CV curves of Au-CNFs in 0.5 M H_2SO_4 in different scan rates. The redox currents of Au-CNFs modified SPE is gradually increase from 20 mV s^{-1} to 100 mV s^{-1}.

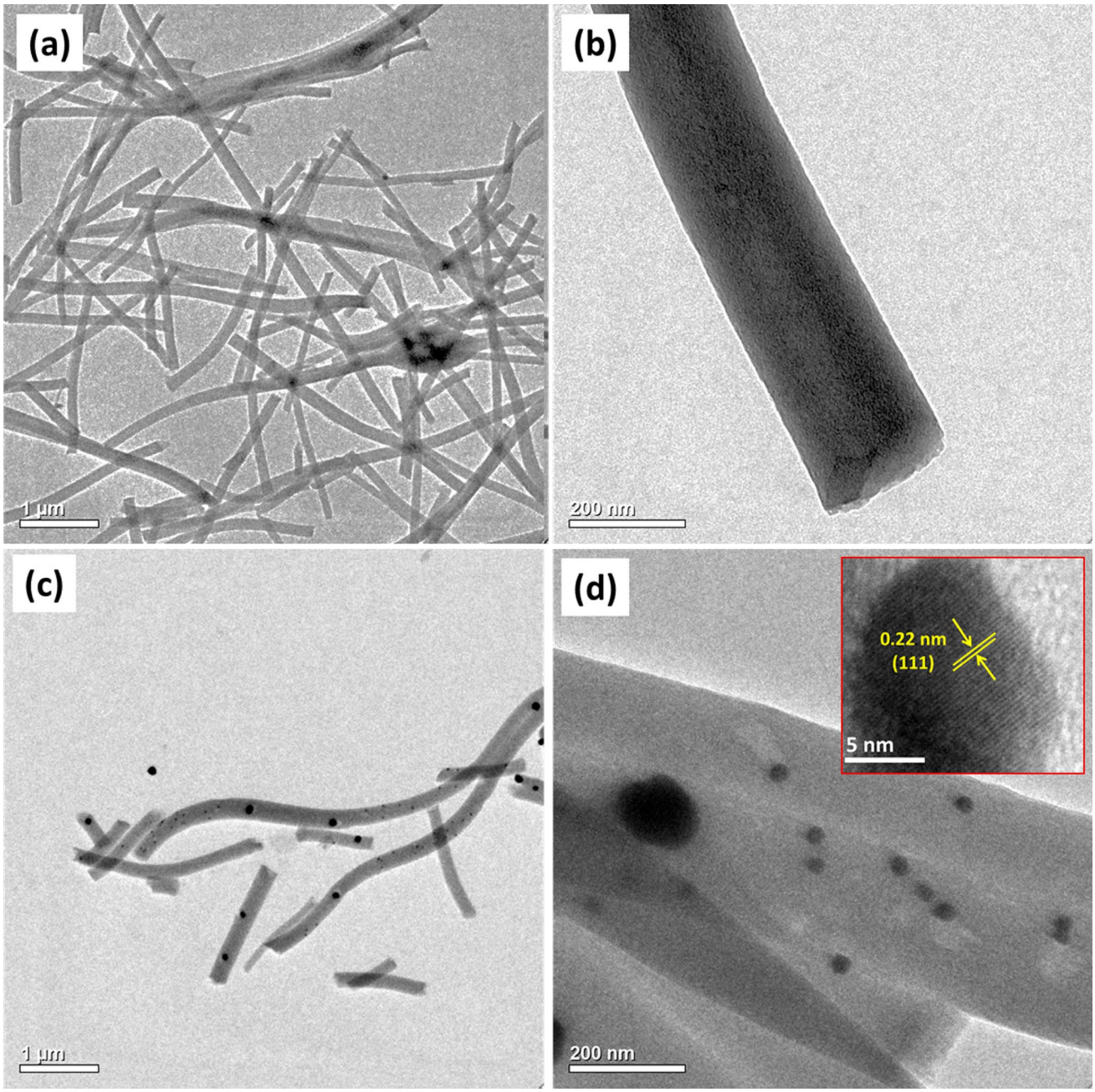

Fig. 3 TEM images of **a** & **b** CNFs and **c** & **d** Au-CNFs and Insert **d** HR-TEM image of Au-CNFs

The EIS technique was used to evaluate the modified electrode's interfacial charge transfer properties. Figure 4c shows the EIS results of CNFs/SPE and Au-CNFs/SPE with a solution of 0.5 M H_2SO_4 in the range of 100 kHz to 100 mHz. It was well understood that the typical impedance spectrum consisted of half-circle and a straight-line section. At higher frequencies, the half-circle radius represented the charge transferring resistance (Rct), whereas at lower frequencies, the linear section represented the diffusing mechanism [50]. The Au-CNFs/SPE exhibited a smaller semicircle charge transfer resistance (Rct) (7.1 Ω) compared to CNFs/SPE (13.2 Ω), suggesting that Au NPs decorated CNFs can enhance electron transfer in bare SPE. Inset Fig. 4c shows the equivalent circuit diagram, which R_1 represents the fluids resistance, R_2 represents the surface resistance, R_3 represents the charge transferring resistance and Q (Q_1 and Q_3) represent the elements constant, respectively [51]. The enhancing effects of Au-CNFs/SPE were greater than those of CNFs/SPE, which can be determined by the high contact at the interface of

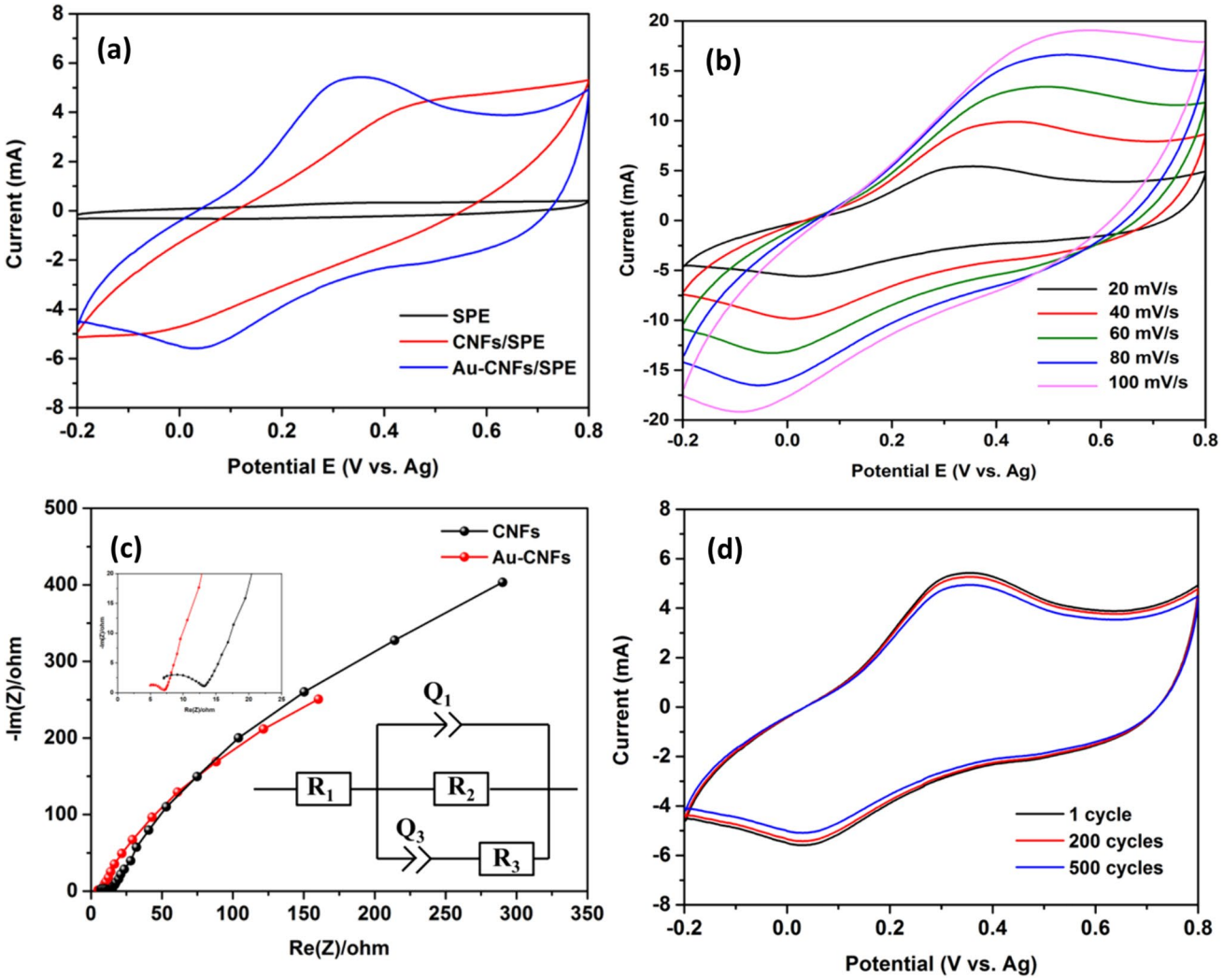

Fig. 4 **a** CV curves of SPE, CNFs/SPE and Au-CNFs/SPE in 0.5 M H_2SO_4 at 20 mVs^{-1}, **b** CV curves of Au-CNFs/SPE in 0.5 M H_2SO_4 at different scan rate of 20, 40, 60, 80 and 100 mVs^{-1}, **c** EIS spectra of CNFs and Au-CNFs and insert shows the equivalent circuit, and **d** CV curve of Au-CNFs/SPE for 500 cycles

electrode and electrolytes. The results reveal that decoration of Au NPs improved the conductivity of CNFs, hence increasing the electrochemical activity.

The electrochemical stability of the Au-CNFs modified SPE was also evaluated using CV. Figure 4d shows the typical CV curves of Au-CNFs/SPE; it is clearly observed that no major decrease in redox peak currents by the increases in number of cycles. However, the Au-CNFs modified SPE electrode shows a minor drop in redox peak currents after 500 cycles, decreasing only 0.48 mA and 0.51 mA, respectively. The observed small drop in redox peak currents is attributed by the dissolving of active materials in the electrolyte throughout the number of cycles. Based on the results, the Au-CNFs/SPE electrode can significantly increase electrochemical stability for analyte oxidation.

3.2 Electrochemical detection of AA, DA, and UA

The developed Au-CNFs/SPE electrochemical sensor towards the oxidation of AA, DA, and UA were explored by voltammetry analysis. The CV curves of SPE and Au-CNFs modified SPE in independent 1 mM of AA, DA and UA as illustrated in Fig. 5. The oxidation of AA, DA and UA on SPE (Fig. 5a) exhibited a weak response due to its poor conductivity, which causes weak electron transport at the electrode–electrolyte interface. The oxidation peaks potential of AA, DA and UA were found at 295, 466 and 531 mV, respectively. It shows that the oxidation peak potential separation of AA, DA and UA has insufficient to bring grate selective behaviour at SPE. After modifying SPE with Au-CNFs (Fig. 5b), the potential peaks of AA, DA and UA were entirely separated as three distinct peaks with

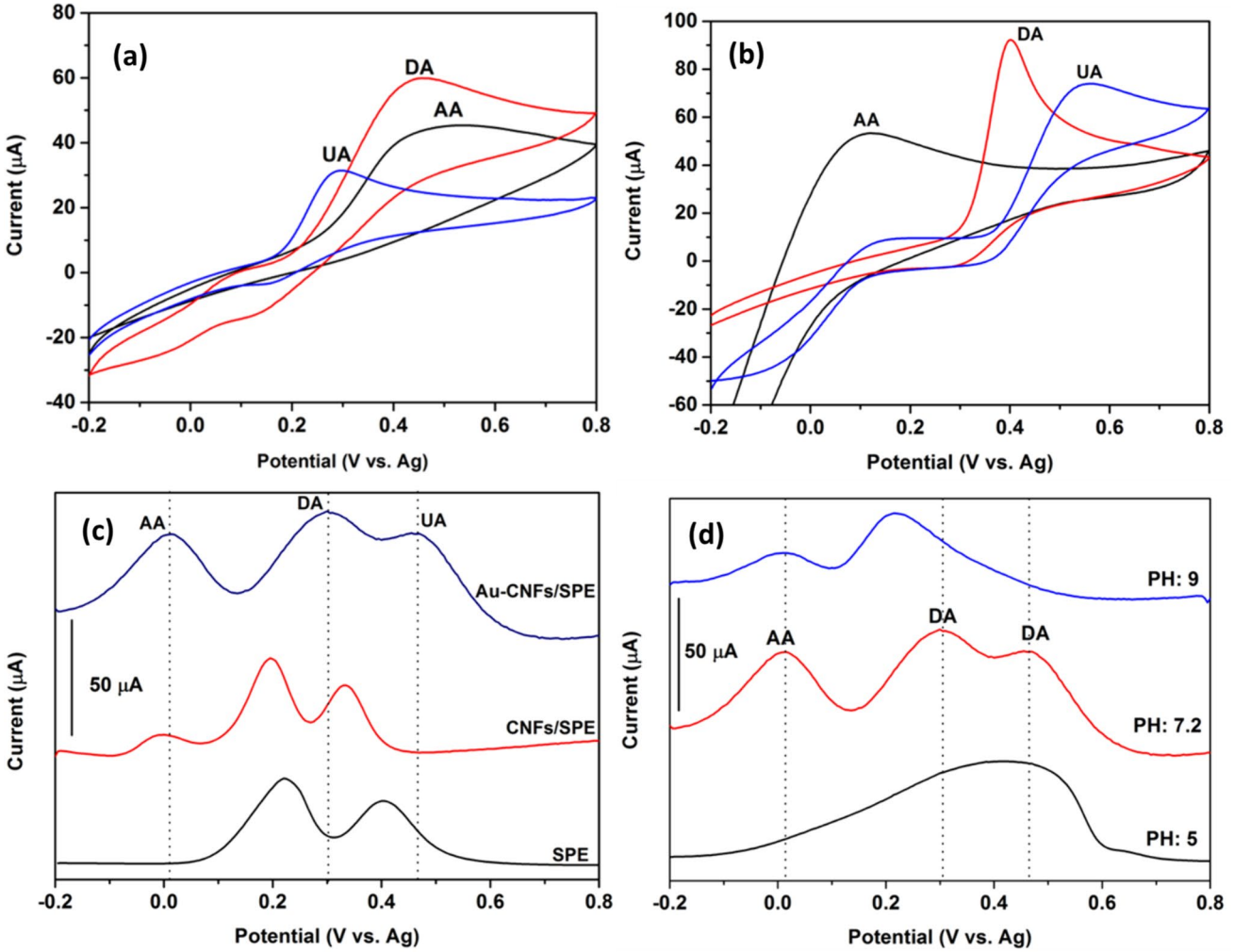

Fig. 5 CV curves for **a** SPE, **b** Au-CNFs/SPE in 0.1 M PBS containing 1 mM of AA, DA and UA at 50 mVs^{-1}, **c** DPV curves of SPE, CNFs/APE and Au-CNFs/SPE in 1 mM ternary mixed of AA, DA and UA and **d** DPV curves of Au-CNFs in different pH. DPV settings: step potential: 5 mV; amplitude: 60 mV; pulse width: 0.05 s; sample width: 0.01 s and pulse period: 0.2 s

high currents. Moreover, the potentials of AA, DA and UA were found at 122, 402 and 561 mV, respectively. This large potential difference is sufficient to distinguish and selective determination of AA, DA and UA. These findings imply the constructed flexible miniature type of Au-CNFs/SPE sensor possesses significant effects on the excellent oxidation of AA, DA and UA.

Furthermore, the effective method of DPV analysis is also used to assess the electrocatalytic activity of Au-CNFs modified SPE towards the oxidation of AA, DA, and UA. The DPV response of SPE, CNFs/SPE, and Au-CNFs/SPE in 0.1 M PBS contained a ternary mixture of 1 mM AA, DA, and UA as displayed in Fig. 5c. The SPE showed the overlapped broad weak oxidation peak at 225 mV, indicating that it is not possible to simultaneous detection of these three analytes. On the contrary, well-defined DPV oxidation peaks were observed at Au-CNFs/SPE with peak potential value of 9 mV, 299 mV and 465 mV for AA, DA and UA, respectively. The separation of electro oxidation peak potential for AA-DA, DA-UA and AA-UA are 290 mV, 166 mV and 456 mV, respectively. The large separation of the peak potentials reveals that the higher electrocatalytic response of Au-CNFs could be employed to develop the biosensor for simultaneous or selective detection. The possible oxidation mechanism of AA, DA, and UA at Au-CNFs/SPE can be described as Scheme 3. Under the experiment condition of pH 7.2, there exists an electrostatic attraction between cationic DA and negative functional groups on the surface of Au-CNFs, which contributes to promote the oxidation of DA to dopamine o-quinone. In addition, the hydroxyl groups of AA, DA, and UA can interact with the oxygen containing functional groups on the surface of Au-CNFs to form hydrogen bonds, which then weakens the hydrogen bonding on the benzene ring of the three substances and promotes

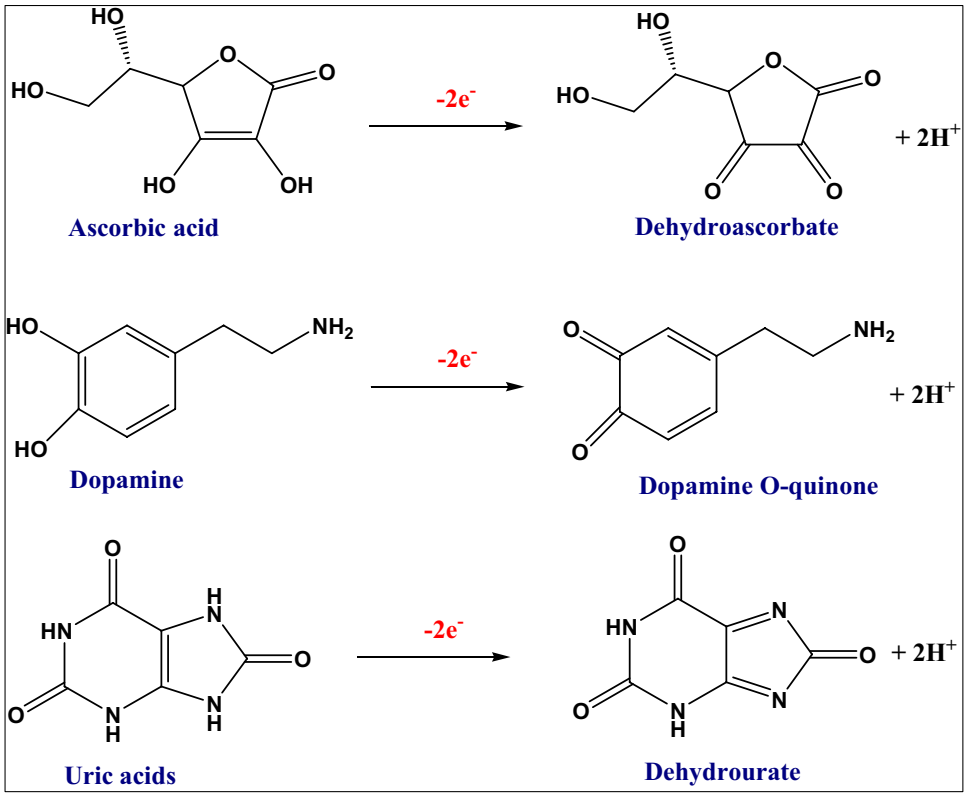

Scheme 3 Schematic illustration for the electro-oxidation mechanism of AA, DA and UA

the oxidation of AA to dehydroascorbate, DA to dopamine o-quinone, and UA to dehydrourate [52].

In the control experiment (Fig. 5c), three distinct oxidation peaks of AA, DA, and UA have been observed in CNFs/SPE at − 4, 195, and 330 mV, respectively. However, as compared to Au-CNFs/SPE, the ascorbic acid peak current is very little, and the DA-UA peak potential separation is very close. The Au NPs decorated CNFs have significantly higher electrochemical activity than bare CNFs owing to their large surface and good conductivity between the electrode interfaces. As a result, the significant electrocatalytic response of Au-CNFs/SPE offers the simultaneous determination of AA, DA and UA.

As seen in Fig. 5d, DPV analysis were used to further examine the impact of electrolyte pH (5 to 9) on the oxidation peak potential of AA, DA and UA at the Au-CNFs/SPE. When the electrolyte pH was less than 6, the analytes oxidation peaks overlapped. Further, the identical oxidation peaks with the potential separation of AA, DA and UA were observed by an increase in electrolyte pH of 7.2 and 9. This implies that ions play a direct role in the entire electrocatalytic activity, i.e., the electro-oxidation process occurs through an electron transfer followed by protonation [53]. Moreover, it is clear that the peak potentials for AA-DA and DA-UA are significantly separated at pH 7.2. As a result, the Au-CNFs modified SPE allows for the individual or simultaneous detection of AA, DA, and UA from their ternary mixture over a wide pH range. According to separation of peak potential as well as sensing response, we chose an electrolyte pH 7.2 for our analysis.

The simultaneous determination of AA, DA, and UA on the Au-CNFs/SPE has been examined using the DPV approach. Figure 6a, c and e shows the DPV curves for particular analyte detection in a ternary mixed solution of AA, DA and UA with one analyte concentration changing while the other two analytes kept constant. The oxidation peak current increases linearly as the specific analyte concentration increased. Meanwhile, Fig. 6b, d and f depicts a linear range between the analytes concentrations versus peak currents. The consequent linear range for AA, DA and UA determination are 5 to 45 µM ($R^2 = 0.9984$), 2 to 16 µM ($R^2 = 0.9962$) and 2 to 16 µM ($R^2 = 0.9983$) with detection limit of 0.9, 0.4 and 0.3 µM ($S/N = 3$), respectively. Also, the relative standard deviation (RSD) obtained were 4.36%, 4.27% and 5.31% for AA, DA, UA, respectively. In the simultaneous determination, the minimal influences of other analytes are occurring while increasing the specific analyte concentration. The comparison of the previously reported electrochemical sensors for the simultaneous determination of AA, DA, and UA and this work is shown in Table 1. It is obvious that Au-CNFs/SPE shows relatively advantage over other reported electrodes at linear range and detection limit. The distinctive structure and electrocatalytic activity of Au-CNFs/

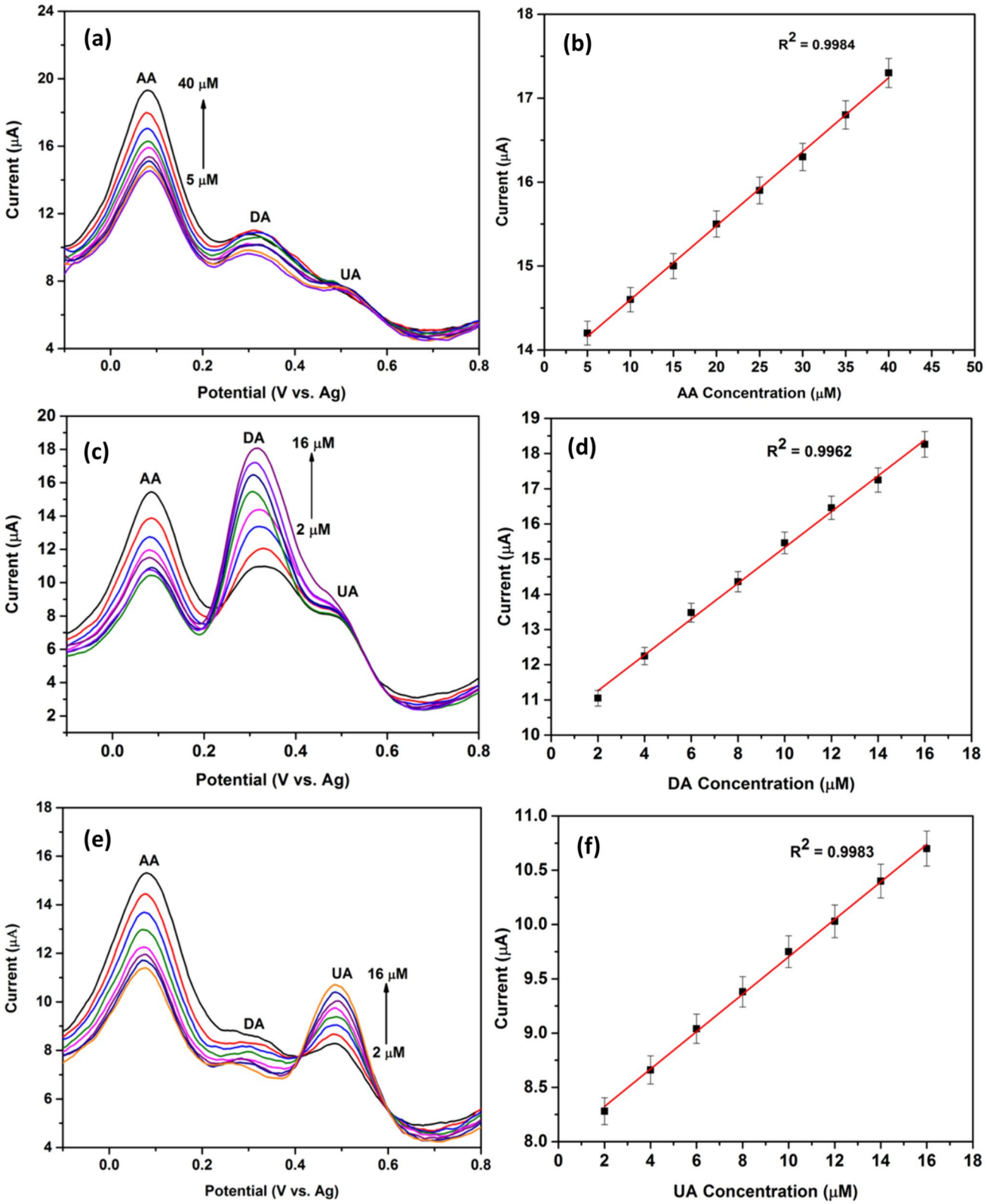

Fig. 6 DPV curves and corresponding linear fit of Au-CNFs/SPE in 0.1 M PBS containing 2 μM DA, 2μ M UA and various concentrations of AA: 5, 10, 15, 20, 25, 30, 35, 40 μM (**a** & **b**), containing 20 μM AA, 2 μM UA and various concentrations of DA: 2, 4, 6, 8, 10, 12, 14, 16 μM (**c** & **d**) and containing 20 μM AA, 2 μM DA and various concentrations of UA: 2, 4, 6, 8, 10, 12, 14, 16 μM (**e** & **f**). DPV settings: step potential: 5 mV; amplitude: 60 mV; pulse width: 0.05 s; sample width: 0.01 s and pulse period: 0.2 s

Table 1 Comparison of different modified electrodes for the simultaneous determination of AA, DA and UA

Electrodes	Linear range (μM)			Detection limit (μM)			Potential separation (mV)			References
	AA	DA	UA	AA	DA	UA	AA-DA	DA-UA	AA-UA	
RGO/AuNPs	10–1000	0.1–100	0.1–100	5.7	0.69	2.2	220	65	285	[54]
AuNPs@GO/PPy/CFP	10–200	0.2–60	2–360	2.4	0.1	1.6	180	120	300	[55]
CTAB–GO/MWCNT/GCE	5–300	5–500	3–60	1	1.5	1	230	80	310	[56]
AuNPs@MoS_2/GCE	20–300	5–200	20–400	3	1	5	–	–	–	[57]
Pt@NP–AuSn/CFP	200–2000	1–10	25–800	5.51	0.13	0.67	134	158	292	[58]
GO–PANI/GCE	150–850	2–14	2–16	50	0.5	1.0	250	190	440	[59]
PdNPs/rGO/GCE	500–3500	3–15	300–1400	100	1	16.67	–	–	–	[60]
PANI–GO/GCE	25–200	2–18	2–18	20	0.5	0.2	320	230	550	[61]
Au–CNFs/SPE	5–40	2–16	2–16	0.9	0.4	0.3	290	166	456	This work

SPE serve as an attractive platform to develop an electrochemical sensor.

The anti-interference ability of modified electrode was investigated by chronoamperometry (CA). Several potential interferential species such as urea, KCl, NaCl, Cu^{2+}, human serum albumin (HAS) and bovine serum albumin (BSA) were selected to evaluate the ability of anti-interference. CA measurement was carried out in 0.1 M PBS at a constant potential of + 0.5 V with addition of analytes and interferents as shown in Fig. 7a. It was found that the existence of aforementioned species showed negligible interferences for simultaneous detection of AA, DA, and UA, revealing a good selectivity of Au-CNFs/SPE. The stability of Au-CNFs/SPE is evaluated by continuous current response of 10 μM AA, 10 μM DA and 10 μM UA in 0.1 M PBS, respectively, for 2000s as shown in Fig. 7b. The applied potentials for the three analytes are 0.01 V, 0.3 V and 0.4 V for AA, DA and UA, respectively. The current signals of the three substances remain basically unchanged within 2000s, indicating that the sensor has good long-term stability. The reproducibility and repeatability of the Au-CNFs/SPE were investigated by DPV in a ternary mixture of 20 μM AA, 20 μM DA and 20 μM UA. To confirm reproducibility, the oxidation of AA, DA and UA was examined separately using five individual measurements on different Au-CNFs/SPE prepared independently. Further, Ten measurements of Au-CNFs/SPE were taken every 2 days for 3 weeks, with each test stored at 4 ℃ to assess repeatability (Fig. 7c and d). The RSD percentage of AA, DA and UA are 1.81, 1.76 and 2.59% in repeatability, and 2.14, 1.69 and 2.72% in reproducibility analysis, respectively. These results show acceptable reproducibility and repeatability for Au-CNFs modified SPE electrode.

4 Conclusion

In summary, a sensitive and cost effective sensor was developed based on Au-CNFs/SPE for simultaneous detection of AA, DA and UA in ternary mixture. The Au NPs decorated CNFs were prepared using an electrospinning approach and followed by a carbonization process. The Au-CNFs modified SPE have an excellent electrochemical performance towards the simultaneous detection of AA, DA and UA with high oxidation currents and well-separated peaks in DPV measurements. The corresponding peak separations were 290 mV (AA – DA), 166 mV (DA – UA), and 456 mV (UA – AA). The linear response of AA, DA and UA in DPV analysis over the range of 5–40 μM, 2–16 μM and 2–16 μM with corresponding detection limits of 0.9 μM, 0.4 μM and 0.3 μM at $S/N = 3$, respectively. Also, the significant properties of Au-CNFs modified SPE exhibits quick electrocatalytic responses with an improved potential separation. Consequently, the specific or simultaneous determination of AA, DA and UA on Au-CNFs/SPE could be observed with improved sensitivity, repeatability, and reproducibility. The current study reveals that Au-CNFs/SPE is a promising approach to develop simultaneous electrochemical biosensors.

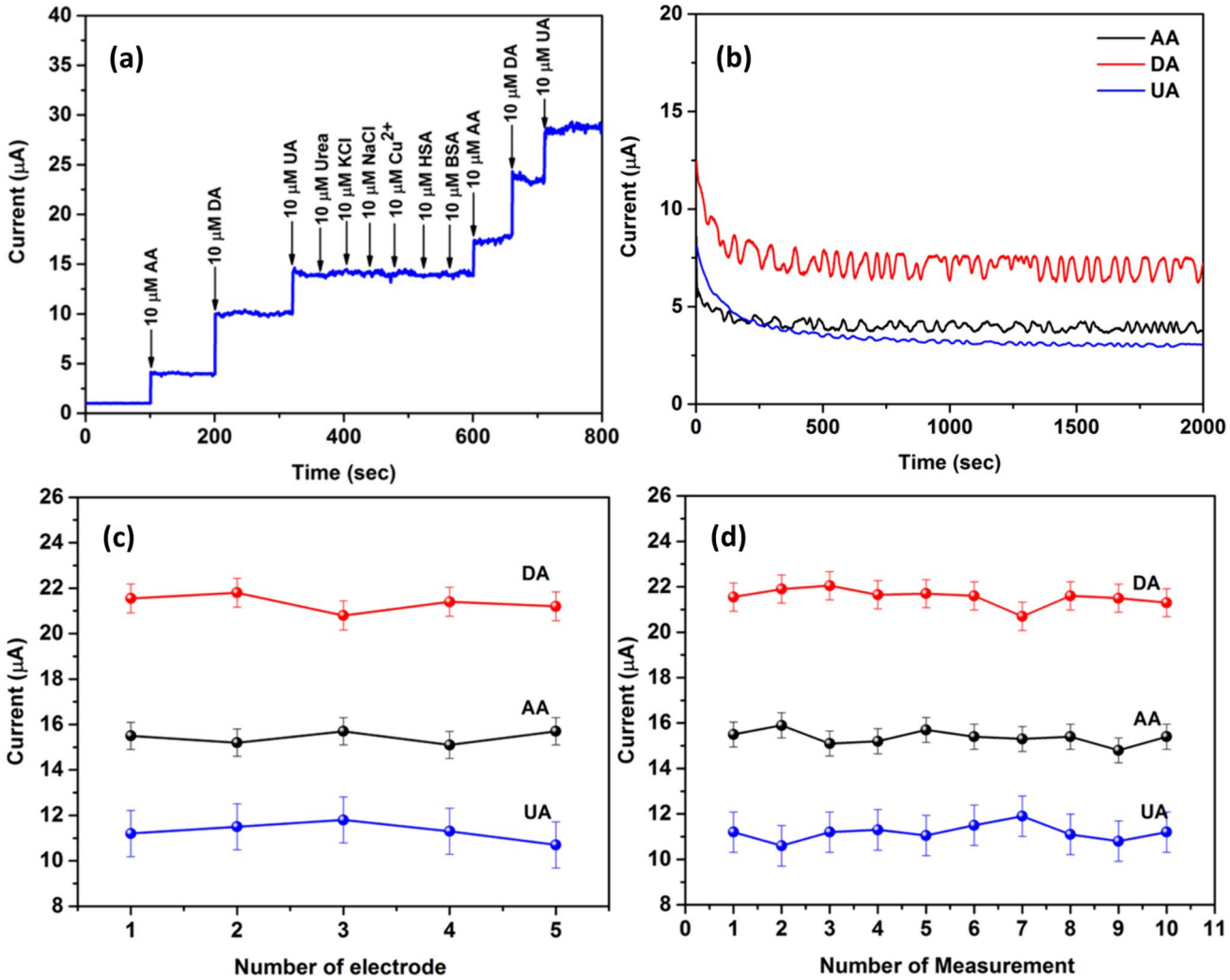

Fig. 7 **a** CA responses of Au-CNFs/SPE with successive addition of 10 μM AA, 10 μM DA, 10 μM UA, and several potential interference into 0.1 M PBS (pH 7.0), **b** CA responses for stability of 10 μM AA, 10 μM DA, 10 μM UA in 0.1 M PBS detected by Au-CNFs/SPE, **c**, **d** DPV peak current of Au-CNFs/SPE obtained in 20 μM AA, 20 μM DA and 20 μM UA for reproducible and repeatable test, respectively

Data availability The datasets used and/or analyzed during the current study are available from the corresponding author on reasonable request.

Declarations

Conflict of interest The authors declare that they have no conflict of interest.

References

1. Su CH, Sun CL, Liao YC (2017) Printed combinatorial sensors for simultaneous detection of ascorbic acid, uric acid, dopamine, and nitrite. ACS Omega 2:4245–4252. https://doi.org/10.1021/acsomega.7b00681
2. Zhang J, Cao T, Zhou Y, Dong L, Zhang H, Liu L, Tong Z (2024) Design and fabrication of NiMn layered double hydroxide/reduced graphene oxide as electrochemical sensor for simultaneous detection of ascorbic acid, dopamine and uric acid. J Inorg Organomet Polym. https://doi.org/10.1007/s10904-024-03027-1
3. Tang S, Liang A, Liu M, Wang W, Zhang F, Luo A (2023) A glassy carbon electrode modified with a composite consisting of electrodeposited chitosan and carboxylated multi-walled carbon nanotubes for simultaneous voltammetric determination of dopamine, serotonin and melatonin. Carbon Lett 33:2129–2139. https://doi.org/10.1007/s42823-023-00556-6
4. Ping J, Wu J, Wang Y, Ying Y (2012) Simultaneous determination of ascorbic acid, dopamine and uric acid using high-performance screen-printed graphene electrode. Biosens Bioelectron 34:70–76. https://doi.org/10.1016/j.bios.2012.01.016
5. Zhang Y, Yuan R, Chai Y, Li W, Zhong X, Zhong H (2011) Simultaneous voltammetric determination for DA, AA and NO_2^- based

on graphene/poly-cyclodextrin/MWCNTs nanocomposite platform. Biosens Bioelectron 26:3977–3980. https://doi.org/10.1016/j.bios.2011.03.017
6. Mallesha M, Manjunatha R, Nethravathi C, Suresh GS, Rajamathi M, Melo JS, Venkatasha TV (2011) Functionalized-graphene modified graphite electrode for the selective determination of dopamine in presence of uric acid and ascorbic acid. Bioelectrochemistry 81:104–108. https://doi.org/10.1016/j.bioelechem.2011.03.004
7. Mu C, Lu H, Bao J, Zhang Q (2018) Visual colorimetric 'turn-off' biosensor for ascorbic acid detection based on hypochlorite-3,3′,5,5′,-Tetramethylbenzidine system. Spectrochim Acta A Mol Biomol Spectrosc 201:61–66. https://doi.org/10.1016/j.saa.2018.04.059
8. Fazio E, Spadaro S, Bonsignore M, Lavanya N, Sekar C, Leonardi SG, Neri G, Neri F (2018) Molybdenum oxide nanoparticles for the sensitive and selective detection of dopamine. J Electroanal Chem 814:91–96. https://doi.org/10.1016/j.jelechem.2018.02.051
9. Rohani T, Taher MA (2018) Novel functionalized multiwalled carbon nanotube-glassy carbon electrode for simultaneous determination of ascorbic acid and uric acid. Arab J Chem 11:214–220. https://doi.org/10.1016/j.arabjc.2014.12.039
10. Sharma A, Singh A, Khosla A, Arya S (2021) Preparation of cotton fabric based non-invasive colorimetric sensor for instant detection of ketones. J Saudi Chem Soc 25:101340. https://doi.org/10.1016/j.jscs.2021.101340
11. Khan S, Arya S, Kumar S, Lehana P (2015) Fabrication and characterization of highly sensitive ZnO/Si SAW device with Pd selective layer for F_2 gas sensing. Microsyst Technol 21:2011–2017. https://doi.org/10.1007/s00542-014-2277-6
12. Singh A, Sharma A, Sundramoorthy AK, Arya S (2023) Quantifying ethanol in sweat with a wearable Al-doped NiO electrode and data analysis. IEEE Sens J 23:22153–22160. https://doi.org/10.1109/JSEN.2023.3304978
13. Dubey A, Singh A, Sharma A, Sundramoorthy AK, Mahadeva R, Gupta V, Dixit S, Arya S (2023) Preparation of Ag doped MgO for electrochemical sensing and degradation of the resorcinol. Appl Phys A 129:692. https://doi.org/10.1007/s00339-023-06972-9
14. Singh A, Sharma A, Arya S (2023) Electrochemical sensing of ascorbic acid (AA) from human sweat using Ni–SnO_2 modified wearable electrode. Inorg Chem Commun 152:110718. https://doi.org/10.1016/j.inoche.2023.110718
15. Bagheri H, Pajooheshpour N, Jamali B, Amidi S, Hajian A, Khoshsafar H (2017) A novel electrochemical platform for sensitive and simultaneous determination of dopamine, uric acid and ascorbic acid based on Fe_3O_4 single bond SnO_2 single bond Gr ternary nanocomposite. Microchem J 131:120–129. https://doi.org/10.1016/j.microc.2016.12.006
16. Mahshid S, Li C, Mahshid SS, Askari M, Dolati A, Yang L, Luo S, Cai Q (2011) Sensitive determination of dopamine in the presence of uric acid and ascorbic acid using TiO_2 nanotubes modified with Pd, Pt and Au nanoparticles. Analyst 136:2322–2329. https://doi.org/10.1039/C1AN15021A
17. Wen D, Guo S, Dong S, Wang E (2010) Ultrathin Pd nanowire as a highly active electrode material for sensitive and selective detection of ascorbic acid. Biosens Bioelectron 26:1056–1061. https://doi.org/10.1016/j.bios.2010.08.054
18. Yang L, Huang N, Lu Q, Liu M, Li H, Zhang Y, Yao S (2016) A quadruplet electrochemical platform for ultrasensitive and simultaneous detection of ascorbic acid, dopamine, uric acid and acetaminophen based on a ferrocene derivative functional Au NPs/carbon dots nanocomposite and graphene. Anal Chim Acta 903:69–80. https://doi.org/10.1016/j.aca.2015.11.021
19. Zhang X, Ma LX, Zhang YC (2015) Electrodeposition of platinum nanosheets on C 60 decorated glassy carbon electrode as a stable electrochemical biosensor for simultaneous detection of ascorbic acid, dopamine and uric acid. Electrochim Acta 177:118–127. https://doi.org/10.1016/j.electacta.2015.01.202
20. Arroquia A, Acosta I, García Armada MP (2020) Self-assembled gold decorated polydopamine nanospheres as electrochemical sensor for simultaneous determination of ascorbic acid, dopamine, uric acid and tryptophan. Mater Sci Eng C 109:110602. https://doi.org/10.1016/j.msec.2019.110602
21. Cheng J, Wang X, Nie T, Yin L, Wang S, Zhao Y, Wu H, Mei H (2020) A novel electrochemical sensing platform for detection of dopamine based on gold nanobipyramid/multi-walled carbon nanotube hybrids. Anal Bioanal Chem 412:2433–2441. https://doi.org/10.1007/s00216-020-02455-5
22. Wang Z, Guo H, Gui R, Jin H, Xia J, Zhang F (2018) Simultaneous and selective measurement of dopamine and uric acid using glassy carbon electrodes modified with a complex of gold nanoparticles and multiwall carbon nanotubes. Sens Actuators B Chem 255:2069–2077. https://doi.org/10.1016/j.snb.2017.09.010
23. Silva W, Ghica ME, Brett CMA (2018) Gold nanoparticle decorated multiwalled carbon nanotube modified electrodes for the electrochemical determination of theophylline. Anal Methods 10:5634–5642. https://doi.org/10.1039/C8AY02150C
24. Musa AM, Kiely J, Luxton R, Honeychurch KC (2023) An Electrochemical screen-printed sensor based on gold-nanoparticle-decorated reduced graphene oxide-carbon nanotubes composites for the determination of 17-β estradiol. Biosensors 13:491. https://doi.org/10.3390/bios13040491
25. Sharma V, Singh P, Kumar A, Gupta N (2023) Electrochemical detection of dopamine by using nickel supported carbon nanofibers modified screen printed electrode. Diam Relat Mater 133:109677. https://doi.org/10.1016/j.diamond.2023.109677
26. Sharma V, Getahun T, Verma M, Villa A, Gupta N (2020) Carbon based catalysts for the hydrodeoxygenation of lignin and related molecules: a powerful tool for the generation of non-petroleum chemical products including hydrocarbons. Renew Sust Energ Rev 133:110280. https://doi.org/10.1016/j.rser.2020.110280
27. Ozoemena OC, Shai LJ, Maphumulo T, Ozoemena KI (2019) Electrochemical sensing of dopamine using onion-like carbons and their carbon nanofiber composites. Electrocatalysis 10:381–391. https://doi.org/10.1007/s12678-019-00520-x
28. Sharma V, Bhatia C, Singh M, Singh C, Upadhyaya S, Kishore K (2020) Synthesis, thermal stability and surface activity of imidazolium monomeric surfactants. J Mol Liq 308:113006. https://doi.org/10.1016/j.molliq.2020.113006
29. Joh H, Ha HY, Prabhuram J, Jo SM, Moon SH (2011) Synthesis of Branched Carbon Nanotubes by Carbonization of Solid Polyvinylidene Fluoride Fibers. Carbon 49:4601–4603. https://doi.org/10.1016/j.carbon.2011.06.014
30. Mao X, Yang X, Rutledge GC, Hatton TA (2014) Ultra-wide-range electrochemical sensing using continuous electrospun carbon nanofibers with high densities of states. ACS Appl Mater Interfaces 6:3394–3405. https://doi.org/10.1021/am405461j
31. Wu L, Zhang X, Ju H (2006) Detection of NADH and ethanol based on catalytic activity of soluble carbon nanofiber with low overpotential. Anal Chem 79:453–458. https://doi.org/10.1021/ac061282
32. Domínguez-Aragón A, Conejo-Dávila AS, Zaragoza-Contreras EA, Dominguez RB (2023) Pretreated screen-printed carbon electrode and Cu nanoparticles for creatinine detection in artificial saliva. Chemosensors 11:102. https://doi.org/10.3390/chemosensors11020102
33. Yan M, Zang D, Ge S, Ge L, Yu J (2012) A disposable electrochemical immunosensor based on carbon screen-printed electrodes for the detection of prostate specific antigen. Biosens Bioelectron 38:355–361. https://doi.org/10.1016/j.bios.2012.06.019
34. Zhang Y, Jiang X, Zhang J, Zhang H, Li Y (2019) Simultaneous voltammetric determination of acetaminophen and isoniazid using

MXene modified screenprinted electrode. Biosens Bioelectron 130:315–321. https://doi.org/10.1016/j.bios.2019.01.043
35. Tajik S, Beitollahi H, Jang HW, Shokouhimehr M (2021) A screen printed electrode modified with Fe_3O_4@polypyrrole-Pt core-shell nanoparticles for electrochemical detection of 6-mercaptopurine and 6-thioguanine. Talanta 232:122379. https://doi.org/10.1016/j.talanta.2021.122379
36. Maity D, Minitha CR, Rajendra Kumar RT (2019) Glucose oxidase immobilized amine terminated multiwall carbon nanotubes/reduced graphene oxide/polyaniline/gold nanoparticles modified screen-printed carbon electrode for highly sensitive amperometric glucose detection. Mater Sci Eng C 105:110075. https://doi.org/10.1016/j.msec.2019.110075
37. Shi W, Li J, Wu J, Wei Q, Chen C, Bao N, Yu C, Gu H (2020) An electrochemical biosensor based on multi-wall carbon nanotube-modified screen-printed electrode immobilized by uricase for the detection of salivary uric acid. Anal Bioanal Chem 412:7275–7283. https://doi.org/10.1007/s00216-020-02860-w
38. Shen X, Ju F, Li G, Ma L (2020) Smartphone-based electrochemical potentiostat detection systemusing pedot: pss/chitosan/graphene modified screen-printed electrodes for dopamine detection. Sensors 20:2781. https://doi.org/10.3390/s20102781
39. Kanyong P, Rawlinson S, Davis J (2016) A voltammetric sensor based on chemically reduced graphene oxide-modified screen-printed carbon electrode for the simultaneous analysis of uric acid. Ascorbic Acid and Dopamine Chemosensors 4:25. https://doi.org/10.3390/chemosensors4040025
40. Kavya KV, Muthu D, Varghese S, Pattappan D, Rajendra Kumar RT, Haldorai Y (2022) Glassy carbon electrode modified by gold nanofibers decorated iron metal–organic framework nanocomposite for voltammetric determination of acetaminophen. Carbon Lett 32:1441–1449. https://doi.org/10.1007/s42823-022-00373-3
41. Xu J, Zhong M, Song N, Wang C, Lu X (2023) General synthesis of Pt and Ni co-doped porous carbon nanofibers to boost HER performance in both acidic and alkaline solutions. Chin Chem Lett 34:107359. https://doi.org/10.1016/j.cclet.2022.03.082
42. Zhang J, Jia W, Dang S, Cao Y (2020) Sub-5 nm octahedral platinum copper nanostructures anchored on nitrogen-doped porous carbon nanofibers for remarkable electrocatalytic hydrogen evolution. J Colloid Interface Sci 560:161–168. https://doi.org/10.1016/j.jcis.2019.10.062
43. Tang Q, Li B, Ma W, Gao H, Zhou H, Yang C, Gao Y, Wang D (2020) Fabrication of a double-layer membrane cathode based on modified carbon nanotubes for the sequential electro-Fenton oxidation of p-nitrophenol. Environ Sci Pollut Res 27:18773–18783. https://doi.org/10.1007/s11356-020-08364-5
44. Dwivedi N, Yeo RJ, Satyanarayana N, Kundu S, Tripathy S, Bhatia CS (2015) Understanding the role of nitrogen in plasma-assisted surface modification of magnetic recording media with and without ultrathin carbon overcoats. Sci Rep 5:7772. https://doi.org/10.1038/srep07772
45. Li M, Zhu Y, Song N, Wang C, Lu X (2018) Fabrication of Pt nanoparticles on nitrogen-doped carbon/Ni nanofibers for improved hydrogen evolution activity. J Colloid Interface Sci 514:199–207. https://doi.org/10.1016/j.jcis.2017.12.028
46. Gubitosa J, Rizzi V, Laurenzana A, Scavone F, Frediani E, Fibbi G, Fanelli F, Sibillano T, Giannini C, Fini P, Cosma P (2022) The "End Life" of the grape pomace waste become the new beginning: the development of a virtuous cycle for the green synthesis of gold nanoparticles and removal of emerging contaminants from water. Antioxidants 11:994. https://doi.org/10.3390/antiox11050994
47. Al-Abduljabbar A, Farooq I (2023) Electrospun polymer nanofibers: processing, properties, and applications. Polymers 15:65. https://doi.org/10.3390/polym15010065
48. Du J, Yue R, Ren F, Yao Z, Jiang F, Yang P, Du Y (2013) Simultaneous determination of uric acid and dopamine using a carbon fiber electrode modified by layer-by-layer assembly of graphene and gold nanoparticles. Gold Bull 46:137–144. https://doi.org/10.1007/s13404-013-0090-0
49. Ibrahim H, Temerk Y (2021) A novel electrochemical sensor based on gold nanoparticles decorated functionalized carbon nanofibers for selective determination of xanthine oxidase inhibitor febuxostat in plasma of patients with gout. Sens Actuators B Chem 347:130626. https://doi.org/10.1016/j.snb.2021.130626
50. Zhao Y, Yang Z, Fan W, Wang Y, Li G, Cong H, Yuan H (2020) Carbon nanotube/carbon fiber electrodes via chemical vapor deposition for simultaneous determination of ascorbic acid, dopamine and uric acid. Arab J Chem 13:3266–3275. https://doi.org/10.1016/j.arabjc.2018.11.002
51. Sakthivel P, Ramachandran K, Balraj C, Senthil TS, Manivel P (2024) Low content of Ni-Pt nanoparticles decorated carbon nanofibers as efficient electrocatalyst for hydrogen evolution reaction. J Chem Technol Biotechnol 99:852–862. https://doi.org/10.1002/jctb.7587
52. Wei Y, Xu Z, Wang S, Liu Y, Zhang D, Fang Y (2020) One-step preparation of carbon quantum dots-reduced graphene oxide nanocomposite–modified glass carbon electrode for the simultaneous detection of ascorbic acid, dopamine, and uric acid. Ionics 26:5817–5828. https://doi.org/10.1007/s11581-020-03703-5
53. Sheng ZH, Zheng XQ, Xu JY, Bao WJ, Wang FB, Xia XH (2012) Electrochemical sensor based on nitrogen doped graphene: Simultaneous determination of ascorbic acid, dopamine and uric acid. Biosens Bioelectron 34:125–131. https://doi.org/10.1016/j.bios.2012.01.030
54. Lee CS, Yu SH, Kim TH (2018) One-step electrochemical fabrication of reduced graphene oxide/gold nanoparticles nanocomposite-modified electrode for simultaneous detection of dopamine, ascorbic acid, and uric acid. Nanomaterials 8:17. https://doi.org/10.3390/nano8010017
55. Tan C, Jie Z, Sun P, Zheng W, Cui G (2020) Gold nanoparticle decorated polypyrrole/graphene oxide nanosheets as a modified electrode for simultaneous determination of ascorbic acid, dopamine and uric acid. New J Chem 44:4916–4926. https://doi.org/10.1039/D0NJ00166J
56. Yang YJ, Li W (2014) CTAB functionalized graphene oxide/multiwalled carbon nanotube composite modified electrode for the simultaneous determination of ascorbic acid, dopamine, uric acid and nitrite. Biosens Bioelectron 56:300–306. https://doi.org/10.1016/j.bios.2014.01.037
57. Zou HL, Li BL, Luo HQ, Li NB (2017) 0D–2D heterostructures of Au nanoparticles and layered MoS_2 for simultaneous detections of dopamine, ascorbic acid, uric acid, and nitrite. Sens actuators B Chem 253:352–360
58. Yang H, Zhao J, Qiu M, Sun P, Han D, Niu L, Cui G (2019) Hierarchical bi-continuous Pt decorated nanoporous Au-Sn alloy on carbon fiber paper for ascorbic acid, dopamine and uric acid simultaneous sensing. Biosens Bioelectron 124–125:191–198. https://doi.org/10.1016/j.bios.2018.10.012
59. Bao Y, Song J, Mao Y, Han D, Yang F, Niu L, Ivaska A (2011) Graphene oxide-templated polyaniline microsheets toward simultaneous electrochemical determination of AA/DA/UA. Electroanalysis 23:878–884. https://doi.org/10.1002/elan.201000607
60. Wei Y, Liu Y, Xu Z, Wang S, Chen B, Zhang D, Fang Y (2020) Simultaneous detection of ascorbic acid, dopamine, and uric

acid using a novel electrochemical sensor based on palladium nanoparticles/reduced graphene oxide nanocomposite. Int J Anal Chem. https://doi.org/10.1155/2020/8812443

61. Manivel P, Dhakshnamoorthy M, Balamurugan A, Ponpandian N, Mangalaraja D, Viswanathan C (2013) Conducting polyaniline-graphene oxide fibrous nanocomposites: preparation, characterization and simultaneous electrochemical detection of ascorbic acid, dopamine and uric acid. RSC Adv 3:14428–14437. https://doi.org/10.1039/c3ra42322k